Reinforcing Effects of Graphene Oxide on Portland Cement Paste

Kai Gong, S.M.ASCE[1]; Zhu Pan[2]; Asghar H. Korayem, Ph.D.[3]; Ling Qiu[4]; Dan Li[5]; Frank Collins[6]; Chien Ming Wang[7]; and Wen Hui Duan, A.M.ASCE[8]

Abstract: In this experimental study, the reinforcing effects of graphene oxide (GO) on portland cement paste are investigated. It is discovered that the introduction of 0.03% by weight GO sheets into the cement paste can increase the compressive strength and tensile strength of the cement composite by more than 40% due to the reduction of the pore structure of the cement paste. Moreover, the inclusion of the GO sheets enhances the degree of hydration of the cement paste. However, the workability of the GO-cement composite becomes somewhat reduced. The overall results indicate that GO could be a promising nanofillers for reinforcing the engineering properties of portland cement paste. **DOI: 10.1061/(ASCE)MT.1943-5533.0001125.**

Author keywords: Graphene oxide; Nanocomposite; Thermogravimetric analysis (TGA); Pore structure; Compressive strength.

Introduction

Patented in 1824 by Joseph Aspdin, a bricklayer and mason in Leeds, England, ordinary portland cement (OPC) is the key ingredient of concrete, which is the world's most widely used building material. OPC paste is a brittle material characterized by a weak tensile strength because of the presence of relatively large pores in the paste that may initiate macrocracks (Birchall et al. 1981). Discrete short fibers have been used to control cracking in fiber-reinforced concrete (FRC) to improve its mechanical properties. The postcracking behavior of FRC depends on the crack-bridging capability of the fibers. A wide variety of fibers has been used in the last three decades, including steel, glass, carbon, and synthetic materials (Bentur and Mindess 2006). These fibers, which are usually randomly oriented in the concrete matrix, may not withstand the tensile loadings as effectively as steel reinforcing bars, but they are more closely spaced and are therefore better at controlling cracks. The efficacy of FRC highly depends on both the mechanical properties and the geometry of the fibers employed (Bentur and Mindess 2006).

[1]Graduate Student, Dept. of Civil Engineering, Monash Univ., Melbourne, VIC 3800, Australia.

[2]Postdoc Fellow, Dept. of Civil Engineering, Monash Univ., Melbourne, VIC 3800, Australia.

[3]Dept. of Civil Engineering, Monash Univ., Melbourne, VIC 3800, Australia.

[4]Graduate Student, Dept. of Materials Engineering, Monash Univ., Melbourne, VIC 3800, Australia.

[5]Professor, Dept. of Materials Engineering, Monash Univ., Melbourne, VIC 3800, Australia.

[6]Associate Professor, Dept. of Civil Engineering, Monash Univ., Melbourne, VIC 3800, Australia.

[7]Professor, Engineering Science Programme and Dept. of Civil and Environmental Engineering, National Univ. of Singapore, Kent Ridge, Singapore 119260.

[8]ARC Future Fellow, Dept. of Civil Engineering, Monash Univ., Melbourne, VIC 3800, Australia (corresponding author). E-mail: Wenhui.duan@monash.edu

Note. This manuscript was submitted on August 26, 2013; approved on May 7, 2014; published online on July 16, 2014. Discussion period open until December 16, 2014; separate discussions must be submitted for individual papers. This paper is part of the ***Journal of Materials in Civil Engineering***, © ASCE, ISSN 0899-1561/A4014010(6)/$25.00.

Recent developments of novel nanosize fibers, such as carbon nanotubes (CNTs) and graphene, have opened up new possibilities for improving the strength of cement paste. Pristine CNTs have an amazing Young's modulus of 1 TPa (Salvetat et al. 1999) and tensile strength of 63 GPa (Yu et al. 2000). The aspect ratio of CNTs is typically approximately 1,000 or higher (Wang et al. 2003). Graphene, on the other hand, is a two-dimensional atomic layer of carbon sheet arranged in a regular hexagonal pattern. Pristine graphene has a Young's modulus of 1 TPa and an intrinsic strength of 130 GPa (Lee et al. 2008). Graphene with aspect ratios (planar dimension or thickness) up to 30,000 or higher can be produced (Tung et al. 2008). Compared with traditional fibers, these nanoscale fibers can offer several distinct advantages, namely, higher strength and stiffness, higher aspect ratio, and smaller fiber spacing, that allow them to better prohibit or hinder the development of cracks at the nanoscale level (Konsta-Gdoutos et al. 2010a).

Most studies on nanosize fiber-reinforced cementitious composites have hitherto been focused on CNTs. With the addition of CNTs in cement paste or mortar, substantial enhancement of compressive strength (Li et al. 2005, 2007; Kumar et al. 2012), flexural strength (Li et al. 2005; Konsta-Gdoutos et al. 2010a), Young's modulus (Saez de Ibarra et al. 2006; Konsta-Gdoutos et al. 2010a), and fracture toughness (Tyson et al. 2011) have been reported, although some contradictory results have been reported, which are generally attributed to poor dispersion of CNTs in cement paste (Cwirzen et al. 2008, 2009). In addition to the enhanced mechanical properties, CNTs have been found to accelerate the hydration process (Makar and Chan 2009) and to reduce the porosity of the cement paste (Li et al. 2005). However, the addition of CNTs reduces the workability (Collins et al. 2012) and increases the viscosity (Konsta-Gdoutos et al. 2010b) of fresh cement paste.

Since its advent in 2004, graphene has raised considerable attention as nanoscale reinforcement like CNTs. So far, most research studies on graphene-reinforced composites have focused on polymeric composites (Cai and Song 2009; Liang et al. 2009; Rafiee et al. 2009, 2010; Xu et al. 2009; Yang et al. 2010; Singh et al. 2011; Wang et al. 2011; Bortz et al. 2012), with some attention on ceramic composites (Walker et al. 2011) and metallic composites (Zhou et al. 2009). In these cases, graphene was oxidized in order to have a better dispersion in the matrix. The reinforcing effects

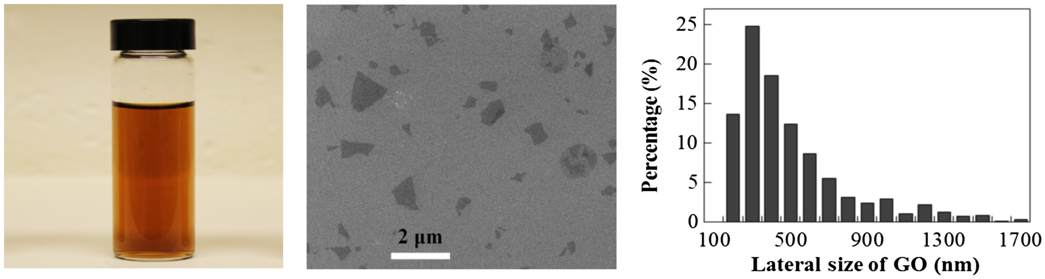

(a) (b) (c)

Fig. 1. (a) Diluted GO solution; (b) SEM image of GO sheets deposited on a piranha-cleaned silicon substrate; (c) histogram for size distribution of GO sheets

of oxidized graphene sheets [generally termed as graphene oxide (GO)] on the mechanical properties of polymers can be even better than those of CNTs. For example, (Rafiee et al. 2010) on an epoxy nanocomposite showed that GO nanofillers require a much lower weight fraction than CNTs in order to achieve a similar degree of reinforcement.

Despite the potential of GO as a nanoscale reinforcement, little attention has been given to reinforcing OPC with GO. In this study, 0.03% by weight GO was incorporated into OPC, and the characteristics of the resultant GO-cement composite were reported with respect to workability, degree of hydration, microstructures, and mechanical strength. A high shear mixer was employed to produce the GO-cement composite in order to improve the distribution of GO in the matrix through input of high shear energy. Because flowability of cement mixture is of great importance in engineering applications, the influence of GO on the workability of fresh cement paste was investigated by using a minislump test. A thermogravimetric analysis (TGA) was performed on hardened cement paste in order to study the effects of GO on its degree of hydration. The porosity and pore size distribution of the GO-cement composite were explored using a mercury intrusion porosimetry (MIP) test. Finally, the influence of 0.03% by weight GO on the compressive strength and tensile strength of cement paste was investigated.

Experimental Study

Materials

GO sheets were synthesized from natural graphite (S-1, Bay Carbon) by using a modified Hummer's method, which mainly involves chemical oxidation of the graphite powder (Hummers and Offeman 1958; Li et al. 2008). The as-produced GO was purified by dialysis for 7 days before being filtrated and dried under vacuum at 60°C for 24 h. The resultant pasty GO was diluted with distilled water and then ultrasonicated for 30 min by using a Branson digital sonicator (VCX750, 750 W, 30% amplitude) to produce stable aqueous GO solution (0.002 g/mL). The resultant GO solution was further diluted with tap water for the production of GO-cement composite with designed concentration. Fig. 1(a) shows a GO solution that remains stable for months without visible precipitation. In order to characterize the size of GO sheets, a scanning electron microscopic (SEM) analysis was performed on diluted GO solution. A typical SEM image is shown in Fig. 1(b). The image shows GO sheets deposited on silicon substrate. By using *Image J*, the surface area of individual GO sheet was measured and used to calculate the approximate lateral size of GO. The size distribution of GO based on more than 500 sheets is shown in Fig. 1(c). The average lateral dimension of GO sheets works out to be approximately 520 × 520 nm, which is much smaller than some values reported in the literature (Tung et al. 2008). This is due to the fact that the size of GO can be influenced by many factors, particularly the path of oxidation and the intensity of ultrasonication (Pan and Aksay 2011). The thickness of a single layer of GO sheet produced is approximately 1 nm according to atomic force microscope measurement (Li et al. 2008). This gives an average aspect (lateral dimension and thickness) ratio of about 520.

Table 1. Chemical Composition of Cement Powder in Percentages

Parameters	Percentages
SiO_2	19.9
Al_2O_3	4.7
Fe_2O_3	3.4
CaO	63.9
MgO	1.3
SO_3	2.6
K_2O	0.5
Na_2O	0.2
Loss on ignition	3
Others	0.5

ASTM Type I (ASTM C150) (ASTM 2012) ordinary portland cement was used in this study. Its chemical composition as determined by X-ray fluorescence is shown in Table 1.

Preparation of Samples

Two mixes of cement paste with a water to cement ratio (w/c) of 0.5 were prepared. One mix was incorporated with 0.03% by weight GO sheets by the weight of cement. The other was a plain cement mix that serves as the reference sample. A high-speed shear mixer (CTE Model 7000) was employed for the mixing to improve the distribution of GO sheets in the matrix. Mixing procedures similar to ASTM C1738-11a (ASTM 2011) were adopted:

- Add the correct amount of GO solution and water to the mixing container and premix the solution at low speed [100–200 revolutions per minute (rpm)] for 15 s to homogenize the solution;
- Add cement powder within a period of 30 s while the mixer is operated at the first preset speed (4,000 rpm) for 60 s;
- Stop the mixer for 30 s, during which any paste that may have collected on the sides of the bowl is scraped down into the hatch; and
- Operate the mixer at the second preset speed (12,000 rpm) for 30 s, stop the mixer for 15 s, and start the mixer at the same speed for an additional 30 s.

After mixing, a portion of the mixtures was used for the minislump test, while the rest of the mixture was cast into molds and vibrated on a vibration table to ensure a good compaction. The molds were then sealed with polyethylene sheets to prevent the escape of moisture. After 24 h, the samples were demolded and cured in a lime-saturated water bath at 20°C.

Testing Procedures

Immediately after mixing, mixtures were poured into a minicore (Fig. 2) to perform the minislump test. The testing procedures used are the same as those adopted by Collins et al. (2012). The purpose of conducting minislump tests is to evaluate the influence of GO sheets on the workability of the cement paste.

In order to examine the effects of GO sheets on the hydration characteristics of cement, a TGA was performed on both mixes at the age of 3, 7, and 28 days. A Mettler Toledo TGA/DSC 1 testing machine was employed for the analysis. In each test, approximately 40–50 mg of sample was heated from 50 to 1,000°C under nitrogen flow at a heating rate of 10°C/min. Three samples were repeated for each test. From the TGA results, two parameters (nonevaporable water content and calcium hydroxide content) were determined. The nonevaporable water content was calculated as the percentage of weight loss recorded from 145 to 1,000°C (Taylor 1997). The calicum hydroxide content was determined by multiplying the percentage of the weight loss recorded between 400 and 600°C by 74/18 [the molar mass ratio of $Ca(OH)_2$ and H_2O] (Mounanga et al. 2004).

An MIP analysis was performed on both mixes in order to investigate the influence of GO sheets on the pore structure of cement. A PoreSizer 9320 porosimeter (Micromeritics) was employed for the test. All test samples were taken from a cement block that had hydrated for 28 days. The samples were then soaked in acetone to stop the hydration and vacuum dried for 5 ± 0.5 days before testing. Each time, 0.5–1 g of sample was used, and three samples were repeated.

In order to examine the influence of GO sheets on the mechanical properties of cement matrix, compression tests and tensile splitting tests were conducted on cylindrical specimens. Small-size specimens (23.5×47 mm) were used due to limits in GO availability. For the compression test, the specimens were tested at the age of 3, 7, and 28 days. The loading rate was set to 0.2 mm/min, which corresponds to approximately 0.3 MPa/s. For the tensile splitting test, the specimens were tested after 28 days' curing. The loading rate was set to 2 kN/ min. Both tests were performed by using an Instron 4204 testing machine with a capacity of 50 kN. At least three samples were repeated for each test.

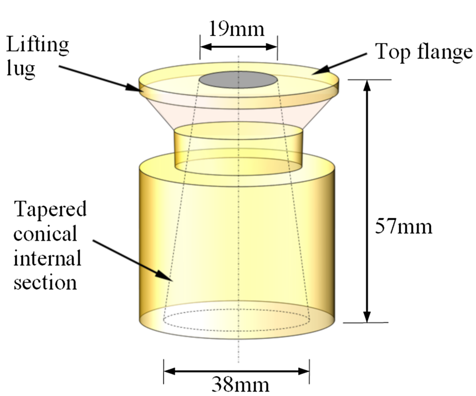

Fig. 2. Geometry of minicore used for minislump test

Results and Discussion

Workability

Fig. 3 shows the minislump flow for the plain cement mixture with 0.03% by weight GO sheets. The minispread diameter of the plain cement sample is approximately 130 mm. When 0.03% by weight GO was added, it is observed that the diameter of minislump is reduced to approximately 85 mm, which is 34.6% lower than that of the plain cement sample. The reduction of minislump diameter shows that GO additives reduce the workability of cement paste. In a previous study, it was also found that small proportions of GO increase both the viscosity and yield stress of fresh cement paste (Gong et al. 2012). The reduction of workability in cement paste due to incorporation of nano additives including CNTs has been widely reported in the literature (Kowald and Trettin 2004; Justice and Kurtis 2007; Senff et al. 2009; Nazari et al. 2010; Collins et al. 2012). It is generally attributed to the large specific surface area of nanomaterials that require more free water to wet their surfaces.

Nonevaporable Water and Calcium Hydroxide

The TGA test results of the nonevaporable water content and the calcium hydroxide content at ages of 3, 7, and 28 days are presented in Figs. 4(a and b), respectively. As expected, both the nonevaporable water content and the calcium hydroxide content in the plain cement samples increase with the age of hydration. It is observed that the nonevaporable water content and the calcium

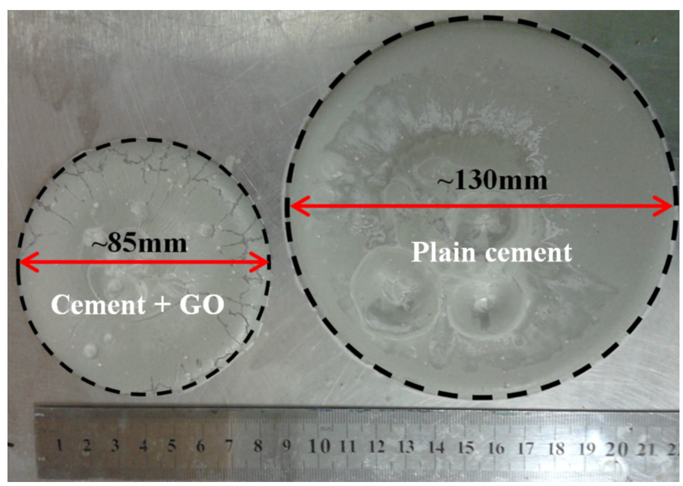

Fig. 3. Minislump flow at 10 min after lifting up the minicore

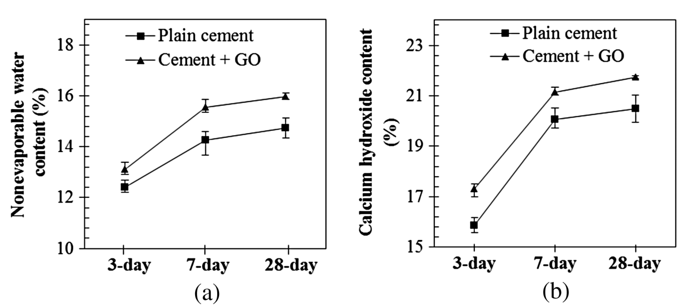

Fig. 4. (a) Nonevaporable water content; (b) calcium hydroxide content in plain cement samples and GO-cement samples at different ages

Table 2. Porosity, Average Pore Diameter, and Total Pore of the Two Mixes at 28 Days

Mixes	Total porosity (%)	Gel pore (<10 nm) (mL/g)[a]	Capillary pore (10 nm–10 μm) (mL/g)[a]	Average pore diameter (nm)	Total pore area (m^2/g)
Plain cement	32.8 ± 0.2	0.022 ± 0.002	0.173 ± 0.003	21.3 ± 1.1	39.7 ± 0.8
GO-cement	28.2 ± 0.7	0.046 ± 0.002	0.125 ± 0.004	13.5 ± 0.2	54.0 ± 1.0

[a]Classified according to Aligizaki (2006).

hydroxide content in the GO-cement samples follow a similar increasing trend as those in the plain cement samples, but they exhibit consistently higher proportions than those in the plain cement sample at all the test ages. At the age of 28 days, the nonevaporable water content and the calcium hydroxide content in the plain cement samples are 14.7 and 20.5%, respectively. With the addition of 0.03% by weight GO, these values are increased by 9 and 6%, respectively. Because both the nonevaporable water content (Parrott et al. 1990; Escalante-Garcia 2003) and calcium hydroxide content (Mounanga et al. 2004) are considered as reliable measurements of the degree of hydration, these results suggest that the addition of GO sheets enhances the degree of hydration of the cement paste at different ages. It has been reported that the addition of GO can increase the degree of crystallinity in polymeric nanocomposite by providing preferential nucleation sites (Das et al. 2009; Xu et al. 2010). Given that cement hydration process is mainly controlled by the nucleation and growth of hydration products, the enhanced degree of hydration in GO-cement composites could also be caused by the nucleation effects of GO.

Porosity and Pore Size Distribution

The results of porosity test for the plain cement samples and the GO-cement samples after 28-day curing are shown in Table 2. It was observed that the use of GO decreases the total porosity of cement paste. With 0.03% by weight GO, the GO-cement composite has a total porosity of 28.2%, which is 13.5% lower than that of its plain cement counterpart. The decrease of porosity could be caused by the improved degree of hydration in the GO-cement samples as shown by the TGA results. It was also observed that the amount of capillary pores (10 nm $< d <$ 10 μm) in the GO-cement samples is 0.173 mL/g, which is 27.7% lower than that of the plain cement. However, the amount of gel pores ($d <$ 10 nm) in the GO-cement sample was found to be more than 100% higher than that of the plain cement. The distributions of pore sizes for both samples can be illustrated using a log differential intrusion curve as shown in Fig. 5. It was observed that the amount of mercury intruded to pores with $d <$ 10 nm is consitently higher in the GO-cement sample, whereas the intrusion to pores with $d >$ 10 nm is consistenly lower in the GO-cement sample. These results show that the presence of GO refines the pore structure of cement paste. Also, the doubling of gel pore volume in the GO-cement samples indicate that more calcium-silicate-hydrate gel may have formed in the GO-cement composite than in the plain cement sample.

The refinement of pore structure is further confirmed by the results of average pore diameter (Table 2), which show that the mean pore diameter of the GO-cement sample is 36.7% finer than that of the plain cement paste. Furthermore, the measurement of specific pore surface area shows that the addition of 0.03% by weight GO increases the total pore area in cement paste by approximately 36%, from 39.7 to 54 m^2/g. This increase may be attributed to the refinement of pore structure and particularly the significant increase of gel porosity in the GO-cement samples.

Compressive and Tensile Strength

Fig. 6 compares a typical compressive stress-strain curve of plain cement specimen with that of the cement-GO composite. It is observed that the use of GO increases not only the failure stress but also the failure strain. The influence of GO on failure stress and strain of cement paste is similar to that of carbon nanotubes reported by Li et al. (2005).

The compressive strengths of cement samples reinforced with GO sheets at different ages are compared with those of plain cement paste in Fig. 7. It was observed that the compressive strengths of both mixes increase with respect to the ages of the samples as expected. The results show that samples reinforced with GO exhibit consistently a higher compressive strength than the plain cement samples at all test ages. At the age of 28 days, the compressive strength of the plain cement sample is 43 MPa. This value is increased by as much as 46% to approximately 63 MPa by having 0.03% by weight GO sheets. Table 3 shows the 28-day tensile strength results obtained from the tensile splitting tests. It was

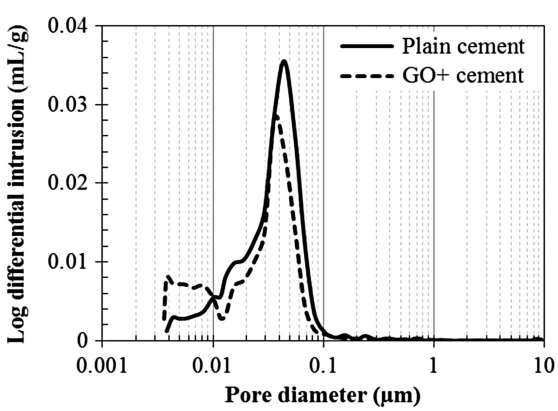

Fig. 5. Pore size distribution for plain cement paste and GO-cement composite

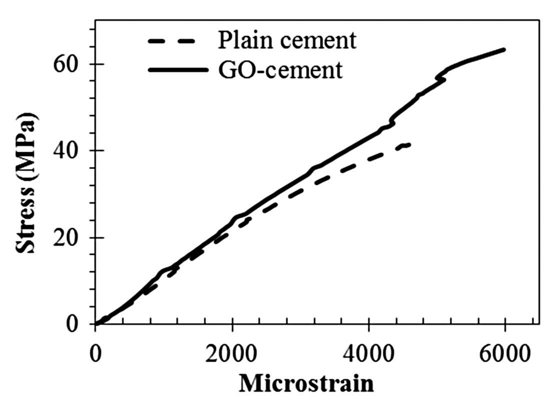

Fig. 6. Typical stress-strain curves for plain cement paste and GO-cement sample

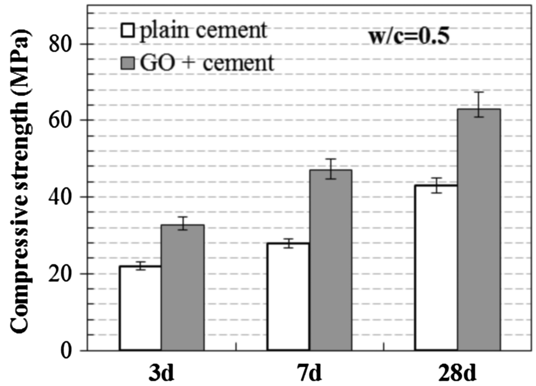

Fig. 7. Compressive strengths for plain cement and GO-cement samples at ages of 3, 7, and 28 days

Table 3. Twenty-Eight-Day Tensile Strength for Both Mixes

Mixes	Tensile strength (MPa)
Plain cement	4.5 ± 0.3
GO-cement	6.9 ± 0.4

Table 4. Comparison of Compressive Strength in Cementitious Nanocomposites Reinforced with CNTs and GO

Source	Matrix	w/c	Type of nanofiber	Concentration (% by weight of cement) (%)	Compressive strength increase (%)
Li et al. (2005)	Mortar	0.45	CNTs	0.5	19 (28-day)
Kumar et al. (2012)	Paste	0.4	CNTs	0.5	15 (28-day)
Cwirzen et al. (2008)	Paste	0.3	CNTs	0.45	50
Present study	Paste	0.5	GO	0.03	46 (28-day)

observed that the tensile strength of the samples reinforced with GO is approximately 50% higher than that of the plain cement sample. The strength gain could be contributed by refinement of pore structure that arises from increase of the degree of hydration, as evidenced by the MIP and TGA results. In addition, GO is a well-established nanosize reinforcement like CNTs, and it has been used to reinforce various polymeric and ceramic matrixes (Singh et al. 2011; Walker et al. 2011). In these matrixes, it is generally recognized that GO and CNTs could suppress crack propagation in the matrixes at nanoscale (Thostenson et al. 2001; Singh et al. 2011). The crack-arresting and bridging effect of CNTs in cement paste has already been reported in the literature (Makar 2011). Therefore, it is expected that GO could arrest and bridge cracks in the cement matrix like CNTs do.

Table 4 compares the reinforcing effect of GO on the strength of cement paste presented in this study with that of CNTs reported in the literature. It is observed that a smaller gain (15–19%) in the 28-day compressive strength of cement mortar or paste was achieved by Li et al. (2005) and Kumar et al. (2012), using much higher concentration of CNTs. Comparing the results achieved using polyacrylic acid polymer-treated multiwall CNTs (Cwirzen et al. 2008), a smaller concentration of GO is required to achieve a similar degree of increase in compressive strength. The superior reinforcing effects of GO over CNTs on the mechanical properties of polymeric matrixes have already been reported (Rafiee et al. 2009, 2010). It was generally attributed to the strong interfacial bonding with the matrix arising from the large specific surface area, highly corrugated surface, and two-dimensional geometry of GO (Singh et al. 2011). The high reinforcing effect of GO on the strength of cement paste make GO a promising reinforcement for cementitious materials.

Conclusions

This paper reports the influence of 0.03% by weight GO (by weight of cement) on the workability, degree of hydration, pore structures, and strength of the OPC paste. The findings can be summarized as follows:

1. Similar to other nanomaterials, i.e., nanosilica and CNTs, the addition of a small proportion of GO sheets reduces the workability of OPC.
2. The use of GO increases the nonevaporable water content and calcium hydroxide content in OPC paste at different test ages. The results indicate that the degree of hydration of OPC paste is enhanced by GO.
3. Cement samples containing GO exhibit 13.5% lower of total porosity, 27.7% smaller amount of capillary pores, and more than 100% larger amount of gel pores than plain cement samples. The refinement of pore structure could be caused by the enhancement in degree of hydration.
4. The addition of GO enhances the strength of OPC paste. The 28-day compressive strength and tensile strength are increased by over 40% with 0.03% by weight GO.

Acknowledgments

The authors are grateful to the Australia Research Council for funding this study. The authors also wish to thank the Monash Centre for Electron Microscopy for the SEM images. The MIP tests were performed at the Department of Chemical Engineering at Monash University with the help of Ms. Kim Phu, and the TGA tests were conducted at the Department of Chemistry at Monash University with support from Mr. Finlay Shanks. The rest of the experiments were conducted at the Department of Civil Engineering at Monash University with the assistance of Mr. Long Goh. Their suggestions and advice are gratefully appreciated.

References

Aligizaki, K. K. (2006). *Pore structure of cement-based materials: Testing, interpretation and requirements*, Taylor and Francis, Milton Park, Abingdon, U.K.

ASTM. (2011). “Standard practice for high-shear mixing of hydraulic cement paste.” *ASTM C 1738*, West Conshohocken, PA, 717–719.

ASTM. (2012). “Standard specification for portland cement.” *ASTM C 150*, West Conshohocken, PA, 157–165.

Bentur, A., and Mindess, S. (2006). *Fibre reinforced cementitious composites*, Taylor and Francis, Milton Park, Abingdon, U.K.

Birchall, J., Howard, A., and Kendall, K. (1981). “Flexural strength and porosity of cements.” *Nat. Lett.*, 289(5796), 388–390.

Bortz, D. R., Heras, E. G., and Martin-Gullon, I. (2012). “Impressive fatigue life and fracture toughness improvements in graphene oxide/epoxy composites.” *Macromolecules*, 45(1), 238–245.

Cai, D., and Song, M. (2009). “A simple route to enhance the interface between graphite oxide nanoplatelets and a semi-crystalline polymer for stress transfer.” *Nanotechnology*, 20(31), 315708.

Collins, F., John, L., and Duan, W. (2012). "The influences of admixtures on the dispersion, workability, and strength of carbon nanotube-OPC paste mixtures." *Cem. Concr. Compos.*, 34(2), 201–207.

Cwirzen, A., Habermehl-Cwirzen, K., Nasibulin, A., Kaupinen, E., Mudimela, P., and Penttala, V. (2009). "SEM/AFM studies of cementitious binder modified by MWCNT and nano-sized Fe needles." *Mater. Charact.*, 60(7), 735–740.

Cwirzen, A., Habermehl-Cwirzen, K., and Penttala, V. (2008). "Surface decoration of carbon nanotubes and mechanical properties of cement/carbon nanotube composites." *Adv. Cem. Res.*, 20(2), 65–73.

Das, B., Eswar Prasad, K., Ramamurty, U., and Rao, C. (2009). "Nano-indentation studies on polymer matrix composites reinforced by few-layer graphene." *Nanotechnology*, 20(12), 125705.

Escalante-Garcia, J. (2003). "Nonevaporable water from neat OPC and replacement materials in composite cements hydrated at different temperatures." *Cem. Concr. Res.*, 33(11), 1883–1888.

Gong, K., et al. (2012). "Rheological behaviours of graphene oxide reinforced cement composite." *ACUN6–Composites and Nanocomposites in Civil, Offshore and Mining Infrastructure*, Monash Univ., Melbourne.

Hummers, W. S., Jr., and Offeman, R. E. (1958). "Preparation of graphitic oxide." *J. Am. Chem. Soc.*, 80(6), 1339.

Image J software, version 1.44e [Computer software]. National Institutes of Health, Bethesda, MD.

Justice, J., and Kurtis, K. (2007). "Influence of metakaolin surface area on properties of cement-based materials." *J. Mater. Civ. Eng.*, 10.1061/(ASCE)0899-1561(2007)19:9(762), 762–771.

Konsta-Gdoutos, M. S., Metaxa, Z. S., and Shah, S. P. (2010a). "Multi-scale mechanical and fracture characteristics and early-age strain capacity of high performance carbon nanotube/cement nanocomposites." *Cem. Concr. Compos.*, 32(2), 110–115.

Konsta-Gdoutos, M. S., Metaxa, Z. S., and Shah, S. P. (2010b). "Highly dispersed carbon nanotube reinforced cement based materials." *Cem. Concr. Res.*, 40(7), 1052–1059.

Kowald, T., and Trettin, R. (2004). "Influence of surface-modified carbon nanotubes on ultrahigh performance concrete." *Proc., Int. Symp. on Ultra High Performance Concrete*, Kassel University Press GmbH, Kassel, Germany, 195–202.

Kumar, S., Kolay, P., Malla, S., and Mishra, S. (2012). "Effect of multi-walled carbon nanotubes on mechanical strength of cement paste." *J. Mater. Civ. Eng.*, 10.1061/(ASCE)MT.1943-5533.0000350, 84–91.

Lee, C., Wei, X., Kysar, J. W., and Hone, J. (2008). "Measurement of the elastic properties and intrinsic strength of monolayer graphene." *Science*, 321(5887), 385–388.

Li, D., Müller, M. B., Gilje, S., Kaner, R. B., and Wallace, G. G. (2008). "Processable aqueous dispersions of graphene nanosheets." *Nat. Nanotechnol.*, 3(2), 101–105.

Li, G. Y., Wang, P. M., and Zhao, X. (2005). "Mechanical behavior and microstructure of cement composites incorporating surface-treated multi-walled carbon nanotubes." *Carbon*, 43(6), 1239–1245.

Li, G. Y., Wang, P. M., and Zhao, X. (2007). "Pressure-sensitive properties and microstructure of carbon nanotube reinforced cement composites." *Cem. Concr. Compos.*, 29(5), 377–382.

Liang, J., et al. (2009). "Molecular-level dispersion of graphene into poly (vinyl alcohol) and effective reinforcement of their nanocomposites." *Adv. Funct. Mater.*, 19(14), 2297–2302.

Makar, J. (2011). "The effect of SWCNT and other nanomaterials on cement hydration and reinforcement." *Nanotechnology in civil infrastructure*, Springer, Berlin, Heidelberg, 103–130.

Makar, J. M., and Chan, G. W. (2009). "Growth of cement hydration products on single-walled carbon nanotubes." *J. Am. Ceram. Soc.*, 92(6), 1303–1310.

Mounanga, P., Khelidj, A., Loukili, A., and Baroghel-Bouny, W. (2004). "Predicting Ca(OH)2 content and chemical shrinkage of hydrating cement pastes using analytical approach." *Cem. Concr. Res.*, 34(2), 255–265.

Nazari, A., Riahi, S., Riahi, S., Shamekhi, S. F., and Khademno, A. (2010). "An investigation on the strength and workability of cement based concrete performance by using ZrO2 nanoparticles." *J. Am. Sci.*, 6(4), 29–33.

Pan, S., and Aksay, I. A. (2011). "Factors controlling the size of graphene oxide sheets produced via the graphite oxide route." *ACS Nano*, 5(5), 4073–4083.

Parrott, L. J., Geiker, M., Gutteridge, W. A., and Killoh, D. (1990). "Monitoring portland cement hydration: Comparison of methods." *Cem. Concr. Res.*, 20(6), 919–926.

Rafiee, M. A., et al. (2010). "Fracture and fatigue in graphene nanocomposites." *Small*, 6(2), 179–183.

Rafiee, M. A., Rafiee, J., Wang, Z., Song, H., Yu, Z. Z., and Koratkar, N. (2009). "Enhanced mechanical properties of nanocomposites at low graphene content." *ACS Nano*, 3(12), 3884–3890.

Saez de Ibarra, Y., Gaitero, J., Erkizia, E., and Campillo, I. (2006). "Atomic force microscopy and nanoindentation of cement pastes with nanotube dispersions." *Physia Status Solidi (a)*, 203(6), 1076–1081.

Salvetat, J.-P., et al. (1999). "Elastic and shear moduli of single-walled carbon nanotube ropes." *Phys. Rev. Lett.*, 82(5), 944–947.

Senff, L., Labrincha, J. A., Ferreira, V. M., Hotza, D., and Repette, W. L. (2009). "Effect of nano-silica on rheology and fresh properties of cement pastes and mortars." *Constr. Build. Mater.*, 23(7), 2487–2491.

Singh, V., Joung, D., Zhai, L., Das, S., Khondaker, S. I., and Seal, S. (2011). "Graphene based materials: Past, present and future." *Prog. Mater. Sci.*, 56(8), 1178–1271.

Taylor, H. F. W. (1997). *Cement chemistry*, Thomas Telford, London.

Thostenson, E. T., Ren, Z., and Chou, T.-W. (2001). "Advances in the science and technology of carbon nanotubes and their composites: A review." *Compos. Sci. Technol.*, 61(13), 1899–1912.

Tung, V. C., Allen, M. J., Yang, Y., and Kaner, R. B. (2008). "High-throughput solution processing of large-scale graphene." *Nat. Nanotechnol.*, 4(1), 25–29.

Tyson, B. M., Abu Al-Rub, R. K., Yazdanbakhsh, A., and Grasley, Z. (2011). "Carbon nanotubes and carbon nanofibers for enhancing the mechanical properties of nanocomposite cementitious materials." *J. Mater. Civ. Eng.*, 10.1061/(ASCE)MT.1943-5533.0000266, 1028–1035.

Walker, L. S., Marotto, V. R., Rafiee, M. A., Koratkar, N., and Corral, E. L. (2011). "Toughening in graphene ceramic composites." *ACS Nano*, 5(4), 3182–3190.

Wang, Y., Shi, Z., Fang, J., Xu, H., and Yin, J. (2011). "Graphene oxide/polybenzimidazole composites fabricated by a solvent-exchange method." *Carbon*, 49(4), 1199–1207.

Wang, Y., Wu, J., and Wei, F. (2003). "A treatment method to give separated multi-walled carbon nanotubes with high purity, high crystallization and a large aspect ratio." *Carbon*, 41(15), 2939–2948.

Xu, J. Z., et al. (2010). "Isothermal crystallization of poly (L-lactide) induced by graphene nanosheets and carbon nanotubes: A comparative study." *Macromolecules*, 43(11), 5000–5008.

Xu, Y., Hong, W., Bai, H., Li, C., and Shi, G. (2009). "Strong and ductile poly (vinyl alcohol)/graphene oxide composite films with a layered structure." *Carbon*, 47(15), 3538–3543.

Yang, X., Tu, Y., Li, L., Shang, S., and Tao, X. (2010). "Well-dispersed chitosan/graphene oxide nanocomposites." *ACS Appl. Mater. Interfaces*, 2(6), 1707–1713.

Yu, M. F., Lourie, O., Dyer, M. J., Moloni, K., Kelly, T. F., and Ruoff, R. S. (2000). "Strength and breaking mechanism of multiwalled carbon nanotubes under tensile load." *Science*, 287(5453), 637–640.

Zhou, X., et al. (2009). "In situ synthesis of metal nanoparticles on single-layer graphene oxide and reduced graphene oxide surfaces." *J. Phys. Chem. C*, 113(25), 10842–10846.